IOP Publishing

Eric Smith and Supriya Krishnamurthy

Chapter 6

Limit cycles and noisy clocks

Evolutionary dynamics can exhibit a new form of classical symmetry breaking possible in non-equilibrium stochastic processes but outside the scope of equilibrium systems. This is the breaking of unique rest points into limit cycles with a continuous phase symmetry, in systems that have only discrete symmetries among the agent types. The classic rock–paper–scissors (RPS) game exhibits this form of symmetry breaking. Such symmetry breaking is possible because in non-equilibrium systems, ordered phases are extended-time trajectories and time translation is a symmetry in addition to the discrete symmetries among agent types. Like symmetries among agent types, time-translation invariance can be hidden in ordered background states that result from dynamics, introducing phenomena associated with continuous symmetry in systems where the type spaces themselves have no such symmetries. Broken time-translation symmetry results in residual population dynamics which is a continuously occurring random walk relative to the uniform phase advance along the limit cycle. This form of group-level motion contrasts with the rare escape events by populations that break discrete symmetries. This model illustrates the calculation of the fluctuation spectrum from chapter 4 in cases when it contains a zero eigenvalue reflecting the presence of the hidden symmetry. The proof that a random walk exists, which is not subject to mean regression, even if all orders of fluctuation corrections are taken into account, is the stochastic version of Goldstone's theorem.

6.1 Simple continuous symmetry breaking and a new role for time in non-equilibrium processes

The sets of ordered population states formed by classical symmetry breaking may be either discrete or continuous and distinct population-level dynamics arises in the two cases. In equilibrium phase transitions, in order for a continuous set of ordered population states to exist, the set of transformations that take one state into another

doi:10.1088/978-0-7503-1137-3ch6

must first have existed as symmetries of the underlying configuration space. In non-equilibrium systems, however, a new form of continuous symmetry breaking becomes not only possible but common. A population process having a finite set of agent types, and only discrete exchange symmetries among them, may still form limit cycles (or even more complex attractors). Along these the population states transform under a continuous symmetry even though no such symmetry is a feature of the agent type space. The source of a continuous symmetry group for population states is the symmetry of *time translation* in the underlying dynamics.

To understand how time translation generates transformations among ordered phases, we must first recognize that in non-equilibrium Markov processes, an ordered phase corresponds to an entire *history* rather than to an instantaneous state. Non-equilibrium systems in which discrete symmetry breaking to rest points resembles equilibrium symmetry breaking make it easy to miss this change of concept, since their ordered histories are just extended-time trajectories at fixed points in type-space. (However, the extended-time character of the history re-asserts itself if we compute probabilities of fluctuations [1–3].) For limit cycles or other dynamically non-trivial backgrounds, recognizing the entire history as the ordered state becomes essential even at the classical level, in order to identify the symmetries relevant to the phase transition. Under shifts of time, limit cycles are extended-time trajectories that are transformed as wholes, as the phase along the cycle is advanced or retarded.

We illustrate the way that time-translation symmetry can be spontaneously broken by dynamics the same as any other symmetry and the distinctive consequences that result from this kind of symmetry breaking, in the example of the classic game of RPS played by three agent types[1]. In the classical replicator equation, the breaking of a single stable population state to a limit cycle takes the form of a supercritical Hopf bifurcation. The part of the large-deviations expression that controls this new kind of symmetry breaking is the second-order fluctuation kernel $S^{(2)}$ in (4.86). The Green's function for diffusive relaxation takes on a zero eigenvalue, whose eigenvector is locally tangent to the limit cycle, reflecting the equivalence of all phases for the cycle as a consequence of the hidden symmetry.

In the classical replicator analysis, the existence of a limit cycle seems unproblematic. In the stochastic analysis, however, where fluctuation effects can feed back to change average dynamics, we are forced to ask whether these corrections might destroy the equivalence of ordered configurations corresponding to different phases around the cycle. After all, the agent types have only a discrete, cyclic permutation symmetry and the cycle itself can be strongly non-linear in the configuration space and in its rate of advance. It is the recognition that the limit cycle is an extended-time trajectory, protected by the underlying time-translation symmetry, which allows us to prove that the fluctuation corrections do not destroy its degeneracy, even though the explicit calculation of these fluctuations to all orders is beyond the scope of our analysis.

[1] We do not take up in this monograph another interesting and more subtle question, which is what determines whether the continuous symmetry of time translation, or only one of the discrete agent-exchange symmetries, will be broken in a particular evolutionary game. That question falls within the domain of bifurcation theory in dynamical systems, which is a large area outside the scope of our topic.

The proof is a stochastic process version of the celebrated result known as Goldstone's theorem in statistical mechanics and field theory. In equilibrium systems, Goldstone's theorem ensures the existence of massless particles, sound waves, or other so-called 'gapless' excitations in the face of stochastic or quantum corrections. In population processes, it ensures the existence of phase noise around the limit cycle as a form of population dynamics that is not subject to mean regression and so persists in populations of arbitrarily large size. The noisy walk around the limit cycle is the multilevel population dynamics for continuous-symmetry breaking, which replaces the rare state-switching dynamics in systems with discrete symmetry breaking. We compute the relation between the diffusivity around the cycle and the rate of mean regression toward the cycle, as an application of the non-equilibrium fluctuation-dissipation theorem developed in equations (4.104)–(4.106) of section 4.4.2.1.

6.1.1 Continuous degeneracy of the order parameter in a game with a discrete type space

The simplest game with a supercritical Hopf bifurcation is the totally-symmetric RPS game [4].[2]

Types are indexed (R,P,S), and the population state is denoted

$$\mathrm{n} \equiv \begin{bmatrix} \mathrm{n_R} \\ \mathrm{n_P} \\ \mathrm{n_S} \end{bmatrix}. \tag{6.1}$$

The normal-form payoff matrix assuming random matching is [7]

$$[a] = \bar{a} \begin{bmatrix} 1 \\ 1 \\ 1 \end{bmatrix} \begin{bmatrix} 1 & 1 & 1 \end{bmatrix} + \begin{bmatrix} & -a & b \\ b & & -a \\ -a & b & \end{bmatrix}. \tag{6.2}$$

This form is uniquely specified, up to the magnitudes of a and b, by antisymmetry of payoffs and invariance under cyclic permutation of the agent types. As in our other simple game models, choosing the number of agent types $D = 3$ provides the simplest non-trivial example and lends itself to illustration with two-dimensional figures. However, all the equations in this chapter extend to larger numbers D of types with cyclic permutation symmetry in the payoff matrix.

The RPS model, like the coordination game, converges to its mean-field limit in all respects except for the accumulation of noise along the limit cycle in the broken-symmetry phase. The bifurcation, within mean-field approximation (MFA), is derived by introducing a radius variable

$$\bar{r}^2 \equiv \frac{\bar{n}_\mathrm{R}^2 + \bar{n}_\mathrm{P}^2 + \bar{n}_\mathrm{S}^2}{N^2} - \frac{1}{D}. \tag{6.3}$$

[2] Similar conclusions apply, however, to a wide variety of stochastic processes with limit cycles and many of these have been developed in reaction–diffusion theory [5, 6].

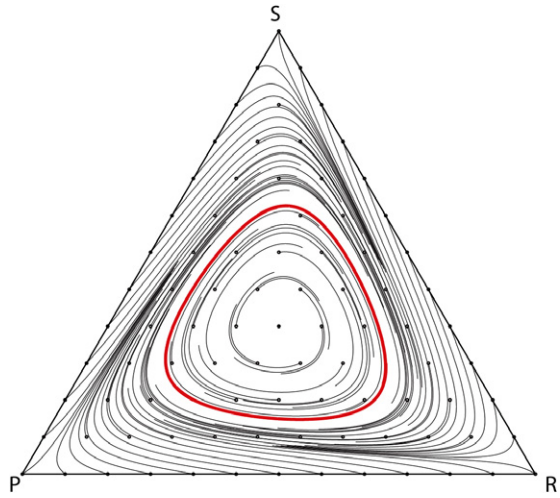

Figure 6.1. Mean-field flow lines for the RPS game (6.2) with the selection parameter $(a - b)N = 24$. The critical population size for this model is $2D^2 = 18$. Dots represent initial mean states $\bar{n}$, and thin black lines are solutions to (2.15) from those initial states. The red line is the limit cycle, to which all solutions converge.

Since the population vector is constrained by $0 \leqslant \bar{n}_R, \bar{n}_P, \bar{n}_S \leqslant N$ and $\bar{n}_R + \bar{n}_P + \bar{n}_S = N$, $\bar{r}^2 = 0$ corresponds to the uniform population $\bar{n}_R = \bar{n}_P = \bar{n}_S = N/D$ and only positive values of $\bar{r}^2$ permit dynamics. Evaluating (2.15) for $\log\ r^2$ gives

$$\frac{\mathrm{d}\log \bar{r}^2}{\mathrm{d}t} = (a - b)N\left[\frac{1}{D} - \frac{2D}{(a - b)N} + O(r) - \bar{r}^2\right]. \tag{6.4}$$

The term denoted $O(r)$ is oscillatory in the angular coordinate on the simplex and does not accumulate over time, as revealed by the simple Floquet analysis in section 6.3.2 below.

From (6.4), $a < b + 2D^2/N$ gives a unique, stable, static equilibrium at $r = 0$ (the uniformly mixed population). When $a > b + 2D^2/N$, the uniform population becomes unstable and all solutions to (2.15) converge to a limit cycle, as shown in figure 6.1. Near the bifurcation, the cycle is approximately circular, with a mean value given by

$$\bar{r}^2 \approx \frac{1}{D} - \frac{2D}{(a - b)N}. \tag{6.5}$$

Symmetric mutation among the D types, which on its own would drive the population toward the uniform distribution, is responsible for the stability of the limit cycle along an interior trajectory. Without mutation the limit cycle would accumulate to the simplex boundary.

6.2 Gaussian-order response and correlation functions

The robust and dynamically important fluctuation effects in this game may all be qualitatively understood and quantitatively approximated to leading order in $1/N$,

from the Gaussian kernel $S^{(2)}$ for fluctuations, introduced in section 4.4.2. The behavior of fluctuations in both the symmetric and symmetry-breaking phases is of interest, along with the quantitative continuation of the spectrum across the transition between phases. We will also illustrate calculation of the Gaussian kernel in both coherent-state and action-angle variables, to show the relation between the two constructions.

We begin with fluctuations about the uniform background, computed in coherent-state variables. We then explain what it means for the limit-cycle order parameter in the broken-symmetry phase to be an extended-time trajectory, show how this leads to differences between non-equilibrium and equilibrium systems and compute the solution for the cycle in the MFA. About this background of the deterministic cycle, we then return and compute the fluctuation spectrum along the radial and tangential directions in action-angle variables, using a weak non-linearity expansion to simplify the limit-cycle coordinates. We show the form of the fluctuation-dissipation theorem that relates mean regression in the radial direction to the rate of accumulation of Brownian noise along the phase of the cycle.

6.2.1 Fluctuations about uniform backgrounds in coherent-state fields

To demonstrate the effect of the terms in the action from section 4.4.2 which control fluctuations, we begin with the expansion about the uniform-population background, where these are constant matrices. We return in section 6.3.1 to the problem of fluctuation expansion about a time-dependent background.

General algebraic forms for the coherent-state expansion are given in appendix 4.6.1. We will keep the number of types D explicit, even though in the examples $D = 3$, to distinguish it from numerical factors related to the order of derivatives and to indicate the scaling of magnitudes with D.

The uniform background satisfies $\bar{\phi}_m = N/D$ for each m. In this background, the diffusion kernel (4.134) evaluates to

$$\overline{\frac{\partial^2 \mathcal{L}}{\partial \phi_i^\dagger \partial \phi_m}} = N\left(\frac{D}{N} + \frac{b-a}{2D}\right)\left(\delta_{im} - \frac{1}{D}\right) - a^A_{im}. \tag{6.6}$$

Continuity in the sum of the eigenvalues about more general backgrounds will also be of interest. From (4.135) and the definition (6.3) of r^2 on the population simplex, we obtain

$$\begin{aligned}\sum_{i=1}^{D} \overline{\frac{\partial^2 \mathcal{L}}{\partial \phi_i^\dagger \partial \phi_i}} &= (D-1)\left[D + N\left(\frac{b-a}{2D}\right)\right] + (D+1)N\left(\frac{a-b}{2}\right)r^2 \\ &\to -2\left|D + N\left(\frac{b-a}{2D}\right)\right|,\end{aligned} \tag{6.7}$$

where in the last line we have used the expression (6.5) for r^2 in the phase with a limit cycle. We will justify this approximation in (6.19) from the Floquet analysis in section 6.3.2 below.

Returning to the uniform background, the noise source corresponding to (6.6), which is the Hessian (4.136), becomes

$$-\overline{\frac{\partial^2 \mathcal{L}}{\partial \phi_i^\dagger \partial \phi_j^\dagger}} = N^2 \left[\frac{3}{D}\left(\bar{a} + \frac{b-a}{2} \right) - \frac{2(b-a)}{D^2} \right] \left(\delta_{ij} - \frac{1}{D} \right). \tag{6.8}$$

The matrix in both equations (which has the same form as the mutation matrix up to a scale factor) is a projector into the transverse simplex $\sum_{m=1}^{D} (\bar{\phi}_m + \phi'_m) = N$. In this simplex, we may diagonalize the diffusive Laplacian by writing the configuration fields ϕ in a suitable basis, similarly to the diagonalization performed for the pitchfork bifurcation in (5.37). Defining

$$v \equiv \frac{1}{2\sqrt{3}} \begin{bmatrix} 2 \\ -1 \\ -1 \end{bmatrix} + \frac{\mathrm{i}}{2} \begin{bmatrix} 0 \\ 1 \\ -1 \end{bmatrix}, \tag{6.9}$$

and v^* to be its complex conjugate, the projection matrix in (6.8) may be written

$$\begin{bmatrix} 1 & & \\ & 1 & \\ & & 1 \end{bmatrix} - \frac{1}{D} \begin{bmatrix} 1 \\ 1 \\ 1 \end{bmatrix} \begin{bmatrix} 1 & 1 & 1 \end{bmatrix} = v v^\dagger + v^* v^T. \tag{6.10}$$

The diffusive Laplacian then has eigenvalue

$$\frac{\partial^2 \mathcal{L}}{\partial \phi^\dagger \partial \phi} v = N \left[\left(\frac{D}{N} + \frac{b-a}{2D} \right) + \mathrm{i} \frac{(b+a)}{2\sqrt{D}} \right] v, \tag{6.11}$$

for v, and the eigenvalue for v^* is the complex conjugate.

About a uniform background both the eigenvalues and eigenvectors are time-independent, so the time-ordered exponential integrals in the Green's functions (4.99, 4.100) reduce to simple scalar exponents in $(t - t')$. These are readily integrated in the formula (4.105) for M_t, in which we can take $t'' \to -\infty$ because all noise is damped. The result is simply to divide the noise source (6.8) by the sum of the eigenvalue in (6.11) and its complex conjugate (one factor from D^R and one from D^A), yielding the expression for the correlation function of ϕ'

$$\left\langle \phi'_i \phi'_l \right\rangle_t = N \frac{\left[3\left(\bar{a} + \frac{b-a}{2} \right) - \frac{2(b-a)}{D} \right]}{\left| a - b - \frac{2D^2}{N} \right|} \left(\delta_{il} - \frac{1}{D} \right). \tag{6.12}$$

If we expand the instantaneous radial coordinate in the RPS simplex about its mean value as $r \equiv \bar{r} + r'$, with $\bar{r}$ satisfying (6.5), we may estimate the fluctuation magnitude for r' in the symmetric phase where $\bar{r} \equiv 0$,

$$\left\langle \left(r'\right)^2 \right\rangle = \frac{2D}{N} \frac{\bar{a} - \dfrac{a-b}{3} + \dfrac{1}{N}}{\left| a - b - \dfrac{2D^2}{N} \right|}. \tag{6.13}$$

Equation (6.13) provides half of the comparison of the analytic calculation for fluctuations against numerical simulation, shown in figure 6.4. The comparison in the broken-symmetry phase will be more complicated because of the limit-cycle background, to which we return shortly.

6.2.2 Symmetries governing the Hopf bifurcation act on a space of histories

The graph of mean-field solutions to the evolutionary game equation for RPS, shown in figure 6.1, makes it difficult to see from symmetry alone why the ordered population state should follow a limit cycle. Why should fluctuations not cause the cycle to get 'stuck' in one of the corners so that the ordered states would respect the point-group symmetry of the type space, breaking to three trigonally symmetric fixed points the way the coordination game broke to two reflection-symmetric fixed points?[3]

Figure 6.2 shows the relevant symmetries of the problem by embedding population states in a three-dimensional space of both types and time. As developed at length in [3], the elementary entities to which non-equilibrium stochastic processes assign probabilities are not single-time configurations, but entire *histories* extended over time. For example, a fixed steady state becomes not merely a point in type-space, but a vertical trajectory in which only the type coordinates are fixed. In figure 6.2, the history representing the limit cycle is a spiral path that winds around the symmetric fixed point and which may be periodically identified in time at integer multiples of the limit-cycle period. The symmetry that transforms different ordered histories is translation in *time* (vertical displacement in the graph). If any particular ordered history is displaced in time by continuous amounts ranging from zero to a full cycle period, the resulting one-parameter family of spiral histories traces out a sleeve in the type-space/time prism. This non-trivial action of time translation is in contrast to what happens to rest points, which are vertical lines that simply transform into themselves under any time displacement. Because the ordered histories

[3] The corresponding difficulty is called the *hierarchy problem* in the quantum field theory of elementary particles and also has counterparts in condensed matter. Its statement is that any property that solutions to classical equations of motion may have, if it is not required to exist by symmetries of the problem, will generically be lost when fluctuation corrections are added to the classical solution. The typical property of interest is masslessness of elementary particles. If particles are not required to have zero mass by some symmetry, not only will they generically have non-zero masses, the masses should be characteristic of the strongest forces with which the particles interact and these are often large. The circumventing of the hierarchy problem is the reason all theories of massless particles are based on either gauge or global symmetries.

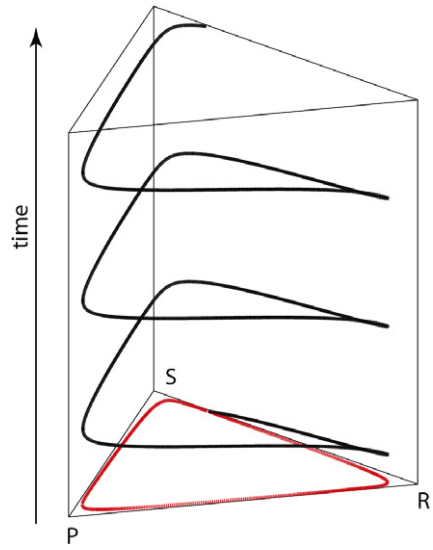

Figure 6.2. The order parameter in a space of histories, corresponding to a limit cycle, is an extended-time path. The projection of the limit cycle onto the space of types is shown in red in the base plane of the graph. Time translation of the spiral trajectory over one cycle period would fill out a non-cylindrical but threefold-symmetric 'sleeve' within the prism shown. This sleeve, which contains the full one-parameter family of ordered backgrounds, is time-independent, reflecting the symmetry hidden by any single background. For a limit cycle near the boundary of the RPS simplex, the cycle slows at the vertices, as shown by vertical inclination of the trajectory. However, because any trajectory winds around the sleeve, while fluctuation effects can change the rate of advance, they cannot collapse the trajectories down to fixed points without changing the topological feature of this winding number.

couple types and time, this translation maps to a rotation in the phase of the projected limit cycle[4].

The sleeve containing all possible phases of the limit cycle *is* transformed into itself by time translation. This is the expression of the fact that the group of ordered states as a whole respect the symmetry that is hidden by any one of them. The *winding number* of any ordered history around the cylindrical sleeve is a topological feature that cannot be continuously deformed into the zero-winding behavior of a set of rest points whose trajectories are mere vertical lines. This topological property is what protects the limit cycle from being a fine-tuned artifact of the classical equations of motion, which might be violated by fluctuation effects. Fluctuation corrections may alter the local speed of advance, smoothly distorting the embedding of the spiral trajectory in time, but they cannot break it into three vertical lines that hide only the point-group symmetry of the type space through anything short of inducing a full topology-changing phase transition.

[4] To appreciate that it is the time translation which is fundamental, note that the time translation acts *uniformly* on the spiraling history. If we wish to project this into an equivalent map on the limit cycle in the base space, the map is not a uniform advance along the line element of the limit cycle, but one that 'stretches' or 'compresses' different segments to reflect the different rates of advance along the cycle.

6.3 Stochastic Goldstone's theorem and noisy clocks

Recall from section 4.4.2.3 that for any stationary path of S, if $\phi^\dagger(t)$, $\phi(t)$ is a solution to $S^{(1)} = 0$, then $\phi^\dagger(t - \delta t)$, $\phi(t - \delta t)$ must also be a solution for any finite δt. The leading term in an expansion of the stationary-path equations (4.87, 4.88) in δt yields the stochastic version of a famous result from field theory known as *Goldstone's theorem* [8]. The mathematical statement of Goldstone's theorem, in terms of representations of symmetry, is that *the generator of the symmetry* hidden by the background (in this case, time translation, or $\mathrm{d}/\mathrm{d}t$), acting on that background, must produce a fluctuation with zero eigenvalue in $S^{(2)}$.

For RPS the theorem states that the cumulant expansion in the distribution for fluctuations has zero-eigenvalue modes corresponding to the direction of symmetry around the limit cycle. We derive only low-order approximations to this cumulant expansion, to produce quantitative estimates for fluctuations transverse to and Brownian motion along the cycle, which we compare to simulations in the next section. It is well understood that low-order approximations to cumulant expansions are not by themselves reliable, especially for exact cancellations such as zero eigenvalues. The hidden symmetry of time translation implies, however, that these zero eigenvalues exist at *all* orders of approximation and even when the approximate expansion in $1/N$ fails to converge, as long as the topological winding number of the average ordered history persists.

The analogy of the limit cycle in RPS to a continuous circle of degenerate ordered states that leads to Goldstone's theorem for equilibrium thermodynamics is limited. Ordinarily time-translation symmetry is not broken by the solutions of equilibrium thermodynamics[5]. Therefore, in order for a continuous symmetry to emerge among spatial ordered states, the potential would need to have the form shown in figure 6.3. The type space of RPS has no such rotational symmetry and the kinematic potential $V(\nu)$ constructed according to the prescription of section 4.4.1.2 shows a single zero, at the unstable rest point for the uniform population. Hence, a grayscale plot for the RPS game analogous to the potential plot for the coordination game in figure 5.3 would show no distinctive contour or other feature at the position of the cycle.

Since the limit-cycle background is a classical solution to the evolutionary game equations of motion, it has $\bar{\phi}^\dagger = 0$ and $\overline{\partial^2 \mathcal{L}/\partial\phi_i \partial\phi_j} \equiv 0$ as well. Therefore the form of (4.115) applicable to the time derivative of the limit cycle is

$$0 = \sum_{j=1}^{D} \left(\delta_{ij} \frac{\mathrm{d}}{\mathrm{d}t} + \overline{\frac{\partial^2 \mathcal{L}}{\partial \phi_i^\dagger \partial \phi_j}} \right) \frac{\mathrm{d}\bar{\phi}_j}{\mathrm{d}t}. \tag{6.14}$$

[5] Ordinarily equilibrium thermodynamics is *defined* through physical context, as a theory of time-independent states. However, the mathematics of equilibrium may readily be extended by analytic continuation to the range of thermodynamically reversible dynamics and systems in this domain may break time-translation symmetry [9, 10]. The paired state of superconductors may also be said to break time translation in the collective phase of the pair wave function, though this is not an observable under most conditions [11].

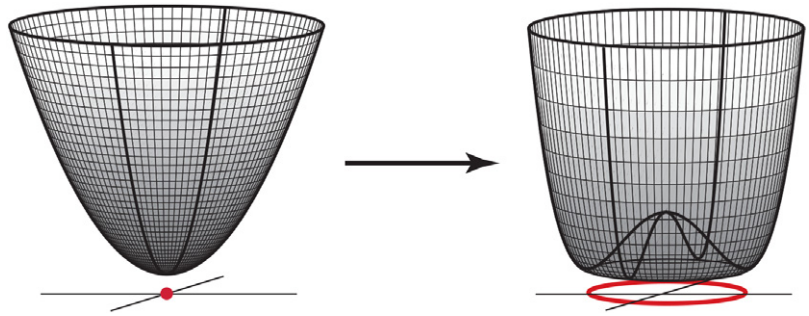

Figure 6.3. Spontaneous symmetry breaking in a two-dimensional equilibrium system. The exact degeneracy of a continuous, one-dimensional loop of solutions (red) requires a rotational symmetry in the underlying potential. Cross-sections of the potential are otherwise equivalent to the one-dimensional case of figure 5.2. The exact degeneracy around the loop in the equilibrium potential ensures that arbitrarily small energies can reach any minimum, independent of the steepness of the mean regression in the radial direction. These most accessible deformations are known as the *Goldstone modes* in the ordered state.

The equivalent form in action-angle variables in the de-scaled time coordinate τ is

$$0 = \sum_{j=1}^{D} \left(\delta_{ij} \frac{\mathrm{d}}{\mathrm{d}\tau} + \overline{\frac{\partial^2 \hat{\mathcal{L}}}{\partial \eta_i \partial \nu_j}} \right) \frac{\mathrm{d}\bar{\nu}_j}{\mathrm{d}\tau}. \tag{6.15}$$

When we transform the vector ν to polar coordinates (r, θ) in the type-simplex, the angular position along the limit cycle will advance as $\mathrm{d}\bar{\theta}/\mathrm{d}\tau \approx$ constant, so (6.15) implies that $\mathrm{d}\bar{\nu}/\mathrm{d}\tau$ is a zero-mode of $\overline{\partial^2 \hat{\mathcal{L}}/\partial \eta_i \partial \nu_j}$ within the same approximation. A zero mode of the matrix that governs mean regression is a collective fluctuation subject to free diffusion.

6.3.1 Frenet coordinates on the limit cycle in the RPS game

A *Frenet coordinate system* on a limit cycle is one whose principle axes are instantaneously tangent and normal to the cycle [5, 6]. These principle axes provide a convenient separation between mean-regressing noise normal to the cycle and Brownian motion tangent to it. For RPS near the bifurcation, the limit cycle is nearly circular and the Frenet coordinates approximate polar coordinates. A *Floquet* analysis integrates properties around cycles, to arrive at the long-time repeated dynamical states or convergence toward them.

Here we compute the leading dependence of the radial coordinate on angle around the cycle and verify that the transformation from polar to Frenet coordinates approaches the identity. By showing that the deviations from circularity are harmonic at leading order, we justify the omission of oscillatory terms in the mean-field radius estimates in section 6.1.1.

Let the normalized radius r introduced in (6.3) and the angle θ in the simplex be polar coordinates for ν. For definiteness, choose $\theta = 0$ to correspond to the

axis $n_R = n_P$. Finally, perform a similar transformation on η to coordinates (h, φ). Thus,

$$\begin{bmatrix} \nu_1 \\ \nu_2 \end{bmatrix} \equiv \begin{bmatrix} r\cos\theta \\ r\sin\theta \end{bmatrix}; \quad \begin{bmatrix} \eta_1 \\ \eta_2 \end{bmatrix} \equiv \begin{bmatrix} h\cos\varphi \\ h\sin\varphi \end{bmatrix}. \tag{6.16}$$

The only combinations of these fields that actually appear in $S^{(2)}$ refer η to the direction of ν, not to the rectilinear frame, so define radial (r) and tangential (t) components of η as

$$\begin{bmatrix} \eta_r \\ \eta_t \end{bmatrix} \equiv \begin{bmatrix} h\cos(\varphi - \theta) \\ h\sin(\varphi - \theta) \end{bmatrix}. \tag{6.17}$$

For small r^2, we will approximate the noise kernel (4.140) by its value in the uniform background for simplicity, because it is not a strong function of ν near the center of the simplex, as was shown in figure 5.4. In polar coordinates, the action to *all orders* in ν and to second order in η then takes a simple form corresponding to the expansion (5.14) used to study stationary points,

$$S \approx N \int d\tau \begin{bmatrix} \eta_r & \eta_t \end{bmatrix} \begin{bmatrix} \dfrac{dr}{d\tau} + \dfrac{\partial \hat{\mathcal{L}}}{\partial \eta_r} \\ r\dfrac{d\theta}{d\tau} + \dfrac{\partial \hat{\mathcal{L}}}{\partial \eta_t} \end{bmatrix} + \frac{1}{2} \begin{bmatrix} \eta_r & \eta_t \end{bmatrix} \frac{\partial^2 \hat{\mathcal{L}}}{\partial \eta^2} \begin{bmatrix} \eta_r \\ \eta_t \end{bmatrix}, \tag{6.18}$$

in which $\partial^2 \hat{\mathcal{L}} / \partial \eta^2$ is computed with respect to the (η_r, η_t) basis.

The stationary point conditions are most easily decomposed in terms of a set of scaling parameters which are functions of the payoffs. The reference scale for radius, $\bar{R}$, will be the value suggested by (6.5),

$$\bar{R}^2 \equiv \frac{1}{D} - \frac{2D}{N(a-b)}. \tag{6.19}$$

The mean rate of advance of the phase θ is

$$\omega = \frac{a+b}{2\sqrt{3}}. \tag{6.20}$$

A normalized radius coordinate will be denoted

$$\rho \equiv \frac{r}{\bar{R}}. \tag{6.21}$$

(The notation here is distinguished from ρ_n used for the original probability density.) Three further combinations of the game parameters appear in the exact stationary point equations:

$$\begin{aligned} A_1 &\equiv \bar{R}^2 \frac{a-b}{2\omega}, \\ 2A_2^2 &\equiv \bar{R}^2 + A_1^2, \\ \tan\alpha &\equiv \frac{1}{3}\frac{a-b}{2\omega}. \end{aligned} \tag{6.22}$$

The small expansion parameter will be $\bar{R}$, in terms of which $A_2 \sim O(\bar{R})$, $A_1 \sim O(\bar{R}^2)$.

Then the stationary point condition for ν in (ρ, θ) coordinates, from the action (6.18), becomes

$$\begin{aligned} \frac{\mathrm{d}\rho}{\omega\,\mathrm{d}\tau} &= -\frac{1}{\bar{R}\omega}\frac{\partial\hat{\mathcal{L}}}{\partial\eta_r} = \rho\Big[A_2\rho\,\sin(3\theta+\alpha) + A_1\big(1-\rho^2\big)\Big] \\ \frac{\rho\,\mathrm{d}\theta}{\omega\,\mathrm{d}\tau} &= -\frac{1}{\bar{R}\omega}\frac{\partial\hat{\mathcal{L}}}{\partial\eta_t} = -\rho\Big[1-\eta_2\rho\,\cos(3\theta+\alpha)\Big] \end{aligned} \tag{6.23}$$

The limit-cycle trajectories are not perfect circles, as shown in figure 6.1 and the angle of inclination to a pure radial vector due to the variation of ρ is

$$\begin{aligned} \frac{\partial\hat{\mathcal{L}}\,/\partial\eta_r}{\partial\hat{\mathcal{L}}\,/\partial\eta_t} = \frac{\dot{\rho}}{\rho\dot{\theta}} &= -\frac{A_2\rho\,\sin(3\theta+\alpha) + A_1\big(1-\rho^2\big)}{1-\eta_2\rho\,\cos(3\theta+\alpha)} \\ &\equiv \tan\xi \\ &\equiv \frac{\mathrm{d}\log\rho}{\mathrm{d}\theta}. \end{aligned} \tag{6.24}$$

These polar coordinates lead to a simple small-parameter expansion if we solve (6.24) for the limit-cycle trajectory, to give

$$\bar{\rho}\big(\bar{\theta}\big) = 1 + \frac{A_2}{3}\cos\big(3\bar{\theta}+\alpha\big) + O\Big(\bar{R}^2\Big) \tag{6.25}$$

At leading order $r = \bar{r}$ around the cycle and the deviation at $O(\bar{r}^2)$ is oscillatory with period three. This term cancels around one cycle, giving the approximate radial convergence equation (6.4).

6.3.2 Gaussian-order fluctuations in the Frenet frame

We may now carry out the derivation parallel to that in section 6.2.1, above the critical point where the stationary solutions for RPS converge on a limit cycle of

non-zero radius. We continue to work in action-angle variables, drawing on algebraic forms provided in appendix 4.6.2.[6]

We begin with the action form for $S^{(2)}$ given in (4.109) with fluctuating fields (η', ν'). In the limit-cycle background, the diffusion kernel $\overline{\partial^2\hat{\mathcal{L}}/\partial\eta\partial\nu}$ is time-dependent and does not generally have any zero entries, which makes direct evaluation of time-ordered exponentials complicated. Yet we know from Goldstone's theorem that the time-derivative of the limit cycle must be a zero mode and we know by symmetry that near the critical point it is approximately a circle. Therefore in the polar coordinates of the previous section, the zero eigenvalue may be made explicit and the resulting lower-triangular form for the kernel makes evaluation of 2×2 time-ordered exponentials elementary. This construction is a simple version of the transformation to a Frenet frame used in [5].

Because the limit cycle is not exactly a circle, we begin with a general invertible transformation V from the rectilinear basis (η^T, ν) to variables $\eta^T V$ and $V^{-1}\nu$. We may always choose V so that

$$\frac{\mathrm{d}V}{\mathrm{d}\tau} + \overline{\frac{\partial^2\hat{\mathcal{L}}}{\partial\eta\partial\nu}}V = V\Lambda, \tag{6.26}$$

for some Λ which is lower triangular, by letting the second column of V be the time derivative of the limit-cycle trajectory. For now, however, assume only that V and Λ are smooth, i.e., $V\Lambda V^{-1}$ has a continuous first derivative so that in the continuum limit the retarded response function becomes

$$\left\langle \nu'_\tau \eta'_{\tau'} \right\rangle = \theta(\tau - \tau')\frac{1}{N} V_\tau \mathcal{T}\left(\mathrm{e}^{-\int_{\tau'}^{\tau}\mathrm{d}u\Lambda_u}\right) V_{\tau'}^{-1}. \tag{6.27}$$

Under the same basis transformation, the correlation function (4.106) at equal times becomes

$$\begin{aligned}\langle \nu'_\tau \nu'_\tau \rangle = {} & V_\tau \mathcal{T}\left(\mathrm{e}^{-\int_{\tau'}^{\tau}\mathrm{d}u\Lambda_u}\right) V_{\tau'}^{-1} \langle \nu'_{\tau'}\nu'_{\tau'} \rangle V_{\tau'}^{-1\dagger} \mathcal{T}^{-1}\left(\mathrm{e}^{-\int_{\tau'}^{\tau}\mathrm{d}u\Lambda_u^*}\right) V_\tau^\dagger \\ & - \frac{1}{N} V_\tau \int_{\tau'}^{\tau} \mathrm{d}z \mathcal{T}\left(\mathrm{e}^{-\int_z^\tau \mathrm{d}u\Lambda_u}\right) V_z^{-1} \overline{\frac{\partial^2\hat{\mathcal{L}}}{\partial\eta^2}}\bigg|_z V_z^{-1\dagger} \mathcal{T}^{-1}\left(\mathrm{e}^{-\int_z^\tau \mathrm{d}u\Lambda_u^*}\right) V_\tau^\dagger. \end{aligned} \tag{6.28}$$

We now construct V through a series of successive approximations, beginning with the transformation (6.16) to static polar coordinates, which may be performed directly within the action.

[6] We note, as an aside, that the correlation function in action-angle variables differs from that in coherent state variables only by corrections of order $1/N$ relative to the leading magnitudes. These arise, as they must, from expectations $\langle\tilde{\phi}\phi'\rangle^2$, which the action-angle correlator includes but the coherent-state correlator does not. The closed-form relation between the noise sources for these two forms, for general payoff matrices, is provided in appendix 4.6.3.

In appendix 6.4 we solve for the matrices V and the fluctuation kernel as an expansion in small r^2 and plug the solutions into the formula (6.28) for the $\nu'\nu'$ correlation function. The result, still using polar coordinates, is that

$$\left\langle \begin{bmatrix} r' \\ \bar{r}\theta' \end{bmatrix} \begin{bmatrix} r' & \bar{r}\theta' \end{bmatrix} \right\rangle_t \to \begin{bmatrix} 0 & \\ & 1 \end{bmatrix} \left\langle \begin{bmatrix} r' \\ \bar{r}\theta' \end{bmatrix} \begin{bmatrix} r' & \bar{r}\theta' \end{bmatrix} \right\rangle_{t'} \begin{bmatrix} 0 & \\ & 1 \end{bmatrix} + \left(\bar{a} - \frac{a-b}{3} + \frac{1}{N} \right) \begin{bmatrix} \frac{D}{2N} \frac{1}{\left| a - b - \frac{2D^2}{N} \right|} & \\ & t - t' \end{bmatrix} + O(\bar{R}). \tag{6.29}$$

Figure 6.4 compares time averages of simulation results for the squared radius $\langle r^2 \rangle$ to these expressions. In the symmetric phase, fluctuations dominate the average and agree closely with the Gaussian-order estimate of (6.13). In the broken-symmetry phase, $\langle r^2 \rangle$ is dominated by the limit cycle itself, which we estimate from numerical simulations of the solutions to the mean-field dynamics (2.15).

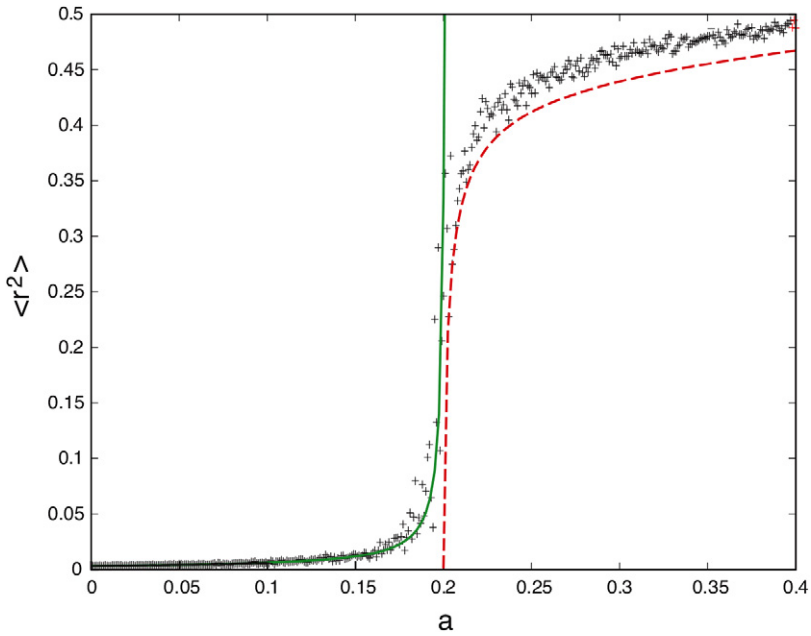

Figure 6.4. Comparison of fluctuation results from analytic estimates and simulations. Time-averaged squared radii $\langle r^2 \rangle$ (crosses), sampled at all a values, are well defined without regard to the circular approximation to the Frenet frame. Equation (6.13) for radial variance in the unbroken phase (green solid) agrees closely. In the broken phase, where most limit cycles are close to the periphery and the Gaussian fluctuation approximation (6.29) is poor, time averages $\langle r^2 \rangle$ over an integer number of limit cycles are computed numerically (red dashed). These underestimate stochastic $\langle r^2 \rangle$ by omission of variance terms. Here $b = 0.2$ and $N = 10000$.

Certain features of this model lead to a rapid transition away from the critical point and into the strongly non-Gaussian regime of fluctuations near the boundary of the simplex, making quantitative comparison to the radial and tangential estimates of (6.29) difficult. If we insert (6.5) for the mean $\bar{r}^2$ on the limit cycle into (6.29) for $\langle (r')^2 \rangle$, we obtain the result that for large N,

$$\left\langle \left(r'\right)^2 \right\rangle \approx \frac{\bar{a}}{\left(2D\bar{r}\right)^2} \tag{6.30}$$

near the critical point, asymptotically independently of N. For the parameters in figure 6.3 and $\bar{a} \sim 1$ (needed so that $\bar{a} \gtrsim a$), $\bar{r}$ only becomes large enough for $\sqrt{\langle (r')^2 \rangle} \ll 1$ near the simplex boundary. At interior positions of the limit cycle, large fluctuations fill most of the simplex. This feature, together with the coordinate singularity at $r = 0$, makes numerical assignment of fluctuations to the Frenet frame ambiguous. The Gaussian approximation for fluctuations is therefore corrected by boundary terms until the limit cycle enters the strongly non-linear regime near the boundary. A thorough treatment of the oscillatory diffusion constants of very similar models in this non-linear regime is given in [5, 6], so we do not duplicate that analysis here.

6.4 Appendix. Rotating backgrounds, polar coordinates and accumulating Brownian noise

In this appendix we construct the Frenet transformation V of section 6.3.2 through a series of successive approximations. The first of these is the conversion (6.16) to polar coordinates, which may be performed directly in the action, and for which the notation of a time-dependent V is not yet needed.

The second-order action (4.109) in polar coordinates becomes

$$S^{(2)} = N \int \mathrm{d}\tau \begin{bmatrix} \eta_\mathrm{r} & \eta_\mathrm{t} \end{bmatrix} \left(\frac{\mathrm{d}}{\mathrm{d}\tau} - \overline{\begin{bmatrix} \frac{\partial \dot{\rho}}{\partial \rho} & \frac{\partial \dot{\rho}}{\rho \partial \theta} \\ \frac{\rho \partial \dot{\theta}}{\partial \rho} & \frac{\partial \dot{\theta}}{\partial \theta} + \frac{\dot{\rho}}{\rho} \end{bmatrix}} \right) \begin{bmatrix} r' \\ \bar{r}\theta' \end{bmatrix} + \frac{1}{2} \begin{bmatrix} \eta_\mathrm{r} & \eta_\mathrm{t} \end{bmatrix} \overline{\frac{\partial^2 \hat{\mathcal{L}}}{\partial \eta^2}} \begin{bmatrix} \eta_\mathrm{r} \\ \eta_\mathrm{t} \end{bmatrix}. \tag{6.31}$$

Having removed most of the frame dependence of the limit cycle with this transformation, we may now return to the systematic approximation of V and Λ as a small parameter expansion. Equation (6.26) becomes

$$\left(\frac{\mathrm{d}}{\mathrm{d}\tau} - \overline{\begin{bmatrix} \frac{\partial \dot{\rho}}{\partial \rho} & \frac{\partial \dot{\rho}}{\rho \partial \theta} \\ \frac{\rho \partial \dot{\theta}}{\partial \rho} & \frac{\partial \dot{\theta}}{\partial \theta} + \frac{\dot{\rho}}{\rho} \end{bmatrix}} \right) V = V \Lambda. \tag{6.32}$$

If we take the time-derivative of the trajectory $(\bar{\rho}, \bar{\theta})$ to be the second column of V, and choose the first column simply to be orthogonal, then

$$\begin{aligned} V &= -\frac{1}{\omega}\overline{\begin{bmatrix} \rho\dot{\theta} & \dot{\rho} \\ -\dot{\rho} & \rho\dot{\theta} \end{bmatrix}} \\ &= \frac{1}{\omega}\overline{\sqrt{\dot{\rho}^2 + (\rho\dot{\theta})^2}}\,\overline{\begin{bmatrix} \cos\xi & \sin\xi \\ -\sin\xi & \cos\xi \end{bmatrix}}, \end{aligned} \tag{6.33}$$

with ξ defined in (6.24). Solving (6.32) then gives

$$\Lambda = \begin{bmatrix} \Lambda^{(11)} & 0 \\ \Lambda^{(21)} & 0 \end{bmatrix}, \tag{6.34}$$

in which

$$\begin{aligned} -\Lambda^{(11)} &= \omega\left[4A_2\bar{\rho}\,\sin\left(3\bar{\theta} + \alpha - 2\bar{\xi}\right) - 2A_1\bar{\rho}^2\cos(2\xi)\right] \\ -\Lambda^{(21)} &= \omega\left[4A_2\bar{\rho}\,\cos\left(3\bar{\theta} + \alpha - 2\bar{\xi}\right) - 2A_1\bar{\rho}^2\sin(2\xi)\right]. \end{aligned} \tag{6.35}$$

Time-ordered exponentials of 2×2 lower-triangular matrices reduce to elementary scalar integrals, as

$$\mathcal{T}\left(\mathrm{e}^{-\int_{\tau 1}^{\tau 2} \mathrm{d}u\Lambda_u}\right) = \begin{bmatrix} \mathrm{e}^{-\int_{\tau 1}^{\tau 2} \mathrm{d}u\Lambda_u^{(11)}} & 0 \\ -\int_{\tau 1}^{\tau 2} \mathrm{d}u\Lambda_u^{(21)}\mathrm{e}^{-\int_{\tau 1}^{u} \mathrm{d}u'\Lambda_{u'}^{(11)}} & 1 \end{bmatrix}. \tag{6.36}$$

V and Λ may be constructed in this way for any stationary solution. Using the solution (6.25) for $\bar{\rho}(\bar{\theta})$, the leading order in V is then

$$V = \begin{bmatrix} 1 & \\ & 1 \end{bmatrix} + O(\bar{R}). \tag{6.37}$$

Thus the polar coordinates turn out to be adequate by themselves. The time-ordered exponential (6.36) similarly simplifies to

$$\mathcal{T}\left(\mathrm{e}^{-\int_{\tau 1}^{\tau 2} \mathrm{d}u\Lambda_u}\right) = \begin{bmatrix} \mathrm{e}^{-2A_1\omega(\tau 1 - \tau 2)} & 0 \\ 0 & 1 \end{bmatrix} + O(\bar{R}). \tag{6.38}$$

Now it remains only to compute the noise kernel. Evaluation of (4.140) about a uniform background gives

$$\begin{aligned} -\frac{\partial^2\hat{\mathcal{L}}}{\partial\eta_i\partial\eta_j} &= -\frac{1}{N^2}\frac{\mathcal{L}}{\partial\phi_i^\dagger\partial\phi_j^\dagger} + \left[\frac{2}{N} + \frac{b-a}{D^2}\right]\left(\delta_{ij} - \frac{1}{D}\right) \\ &= \left[\frac{3}{D}\left(\bar{a} + \frac{b-a}{2}\right) + \frac{2}{N} + \frac{a-b}{D^2}\right]\left(\delta_{ij} - \frac{1}{D}\right). \end{aligned} \tag{6.39}$$

The leading constant correction in small $\bar{R}^2$ can readily be included, leaving out oscillatory terms as they were left out of V in (6.37),

$$\begin{aligned}
-\frac{\partial^2\hat{\mathcal{L}}}{\partial\eta_i\partial\eta_j}\bigg|_{\bar{R}^2\neq 0} &= -\frac{\partial^2\hat{\mathcal{L}}}{\partial\eta_i\partial\eta_j}\bigg|_{\bar{R}^2=0} + \frac{(a-b)}{2D}\bar{R}^2\left(\delta_{ij}-\frac{1}{D}\right) \\
&= -\frac{1}{N^2}\frac{\mathcal{L}}{\partial\phi_i^\dagger\partial\phi_j^\dagger}\bigg|_{\phi_i=N/D} + \left[\frac{1}{N}+\frac{b-a}{2D^2}\right]\left(\delta_{ij}-\frac{1}{D}\right) \\
&= \left[\frac{3}{D}\left(\bar{a}+\frac{b-a}{2}\right)+\frac{1}{N}-\frac{3(b-a)}{2D^2}\right]\left(\delta_{ij}-\frac{1}{D}\right),
\end{aligned} \tag{6.40}$$

but this result differs from (6.39) only by terms of order $1/N$ near the critical point. Now using $D = 3$ for the particular RPS example, the noise kernel (6.40) reduces to the simple expression

$$-\overline{\frac{\partial^2\hat{\mathcal{L}}}{\partial\eta_i\partial\eta_j}} = \left[\bar{a}-\frac{a-b}{3}+\frac{1}{N}\right]\left(\delta_{ij}-\frac{1}{D}\right). \tag{6.41}$$

Incorporating the source (6.41) and the time-ordered exponentials (6.38) in the expression (6.28) for the correlation function, and performing the elementary integrals over $\tau - \tau'$, gives

$$\begin{aligned}
\left\langle\begin{bmatrix} r' \\ \bar{r}\theta'\end{bmatrix}\begin{bmatrix} r' & \bar{r}\theta'\end{bmatrix}\right\rangle_\tau &= \begin{bmatrix} \mathrm{e}^{-2A_1\omega(\tau-\tau')} & \\ & 1\end{bmatrix}\left\langle\begin{bmatrix} r' \\ \bar{r}\theta'\end{bmatrix}\begin{bmatrix} r' & \bar{r}\theta'\end{bmatrix}\right\rangle_{\tau'}\begin{bmatrix} \mathrm{e}^{-2A_1\omega(\tau-\tau')} & \\ & 1\end{bmatrix} \\
&\quad + \left(\bar{a}-\frac{a-b}{3}+\frac{1}{N}\right)\begin{bmatrix} \dfrac{1-\mathrm{e}^{-4A_1\omega(\tau-\tau')}}{4A_1\omega N} & \\ & \dfrac{\tau-\tau'}{N}\end{bmatrix} + O\left(\bar{R}\right).
\end{aligned} \tag{6.42}$$

Restoring the combination of aggregated constants to their expression in terms of the parameters of the problem,

$$4A_1\omega N = \frac{2N}{D}\left(a-b-\frac{2D^2}{N}\right), \tag{6.43}$$

and using large $(\tau - \tau')$ to ignore exponentials in the non-zero damping radial eigenvalue, we obtain (6.29).

Bibliography

[1] Bertini L, De Sole A, Gabrielli D, Jona-Lasinio G and Landim C 2002 Macroscopic fluctuation theory for stationary non equilibrium states *J. Stat. Phys.* **107** 635–75

[2] Bertini L, De Sole A, Gabrielli D, Jona-Lasinio G and Landim C 2009 Towards a nonequilibrium thermodynamics: a self-contained macroscopic description of driven diffusive systems *J. Stat. Phys.* **135** 857–72

[3] Smith E 2011 Large-deviation principles, stochastic effective actions, path entropies, and the structure and meaning of thermodynamic descriptions *Rep. Prog. Phys.* **74** 046601
[4] Hofbauer J and Sigmund K 1998 *Evolutionary Games and Population Dynamics* (New York: Cambridge University Press)
[5] Boland R P, Galla T and McKane A J 2008 How limit cycles and quasi-cycles are related in systems with intrinsic noise *J. Phys. A: Math. Theor.* **41** 435003
[6] Boland R P, Galla T and McKane A J 2009 Limit cycles, complex Floquet multipliers, and intrinsic noise *Phys. Rev.* E **79** 051131
[7] Nowak M A 2006 *Evolutionary Dynamics: Exploring the Equations of Life* (New York: Belknap)
[8] Coleman S 1985 *Aspects of Symmetry* (New York: Cambridge)
[9] Smith E 1998 Carnot's theorem as Noether's theorem for thermoacoustic engines *Phys. Rev.* E **58** 2818–32
[10] Smith E 1999 Statistical mechanics of self-driven Carnot cycles *Phys. Rev.* E **60** 3633–5, PMID: 11970197
[11] Tinkham M 2004 *Introduction to Superconductivity* 2nd edn (New York: Dover)